Appl. Sci. Converg. Technol. 34 (1); 12-15 (2025)
https://doi.org/10.5757/ASCT.2025.34.1.12
eISSN: 2288-6559

Research Paper Check for updates

Thermal Cross-Talk Analysis in Multi-Finger Gallium Nitride High Electron Mobility Transistors

Received 29 November, 2024; revised 9 December, 2024; accepted 12 December, 2024

Junrae Park[a,†], Sung-Jae Chang[b,†], Minsoo Kang[a], Haecheon Kim[a], Ilgyu Choi[b], Hyun-Wook Jung[b], Seong-Il Kim[b], Jong-Won Lim[b], Ho-Kyun Ahn[b,*], and Hyoungsoon Lee[a,c,*]

[a]Department of Intelligent Energy and Industry, Chung-Ang University, Seoul 06974, Republic of Korea
[b]RF/Power Components Research Section, Electronics and Telecommunication Research Institute, Daejeon 34129, Republic of Korea
[c]School of Mechanical Engineering, Chung-Ang University, Seoul 06974, Republic of Korea

[†]These authors contributed equally to this work.

[*]**Corresponding author E-mail: hkahn@etri.re.kr, leeh@cau.ac.kr**

ABSTRACT

The thermal cross-talk in gallium nitride (GaN) high electron mobility transistor (HEMT) multifinger devices is a critical factor that limits their thermal performance, necessitating an in-depth investigation. In this study, the thermal cross-talk according to the number of gate fingers in GaN HEMT devices was analyzed. The number of gate fingers varied from 2 to 24, and the current density was set within a range of 8 W/mm to examine the operating temperatures of the devices. The results showed that the operating temperature of the device increased with higher current density and that the degree of thermal cross-talk was closely related to the number of fingers. When the number of fingers increased, the temperature of the device tended to increase sharply nonlinearly as the current density increased. Furthermore, it was observed that as the number of fingers increased, the temperature difference between the central and edge fingers increased, leading to a degradation in the uniformity of the device's temperature distribution. Additionally, at a low convective heat transfer coefficient, stable operation was impossible because the temperature of the device increased by more than 200 °C, and that for devices with 24 fingers to operate stably below 200 °C, a high convective heat transfer coefficient of 10,000 W/m^2·K or higher is required.

Keywords: Gallium nitride, High electron mobility transistor, Thermal cross-talk, Multi-finger

1. Introduction

Gallium nitride (GaN)-based high electron mobility transistors (HEMTs) have recently attracted considerable interest in power electronics and radio frequency (RF) applications due to their outstanding electrical properties. As a wide bandgap material, GaN exhibits a high breakdown voltage, and thus can be operated under high voltage without performance degradation [1,2]. Additionally, its thermal conductivity compared to conventional silicon-based semiconductors facilitates efficient operation of power devices. These advantages have established GaN HEMTs as essential components in various applications requiring high efficiency and voltage.

Beyond their high breakdown voltage and thermal conductivity, GaN HEMTs also offer high carrier density [3] and electron mobility [4], providing exceptional high-frequency and high-power RF performance. These characteristics make them particularly ideal for RF applications such as power amplifiers, radar systems, and 5 Gbps communication networks [5].

To further enhance the performance of GaN HEMT devices, numerous studies have focused on optimizing various geometric design parameters, such as gate length [6], gate width [7], and the distance between the gate and drain [8]. These studies have provided valuable insights into improving the electrical performance of devices. Most of these studies have focused on devices with 2 – 4 fingers, which relatively simple and easy to manufacture. However, a multi-finger structure is essential to implement high-power and high-frequency devices required for applications such as RF amplifiers and converters. Nevertheless, 2 – 4 finger devices fail to capture the complex interactions such as thermal cross-talk. Consequently, there is a limited understanding of the thermal characteristics and operating temperature variations associated with an increased number of fingers.

Therefore, this study aims to analyze the thermal cross-talk as a function of the number of fingers in GaN HEMT devices and to investigate the relationship between temperature variations caused by thermal cross-talk and the geometric design of the devices. Through this analysis, we systematically understand the thermal characteristics and mechanisms associated with thermal cross-talk and propose new design directions for improved thermal management.

2. Methods

To analyze the thermal cross-talk phenomenon as a function of the number of gate fingers in GaN-on-silicon carbide (SiC) HEMT devices, we used the COMSOL Multiphysics v6.2 program. The simulation geometry and conditions are shown in Fig. 1. We considered multi-finger GaN-on-SiC devices with 2, 4, 12, and 24 heat sources.

This is an Open Access article distributed under the terms of the Creative Commons Attribution Non-Commercial License (https://creativecommons.org/licenses/by-nc-nd/4.0/) which permits non-commercial use, distribution and reproduction in any medium without alteration, provided that the original work is properly cited.

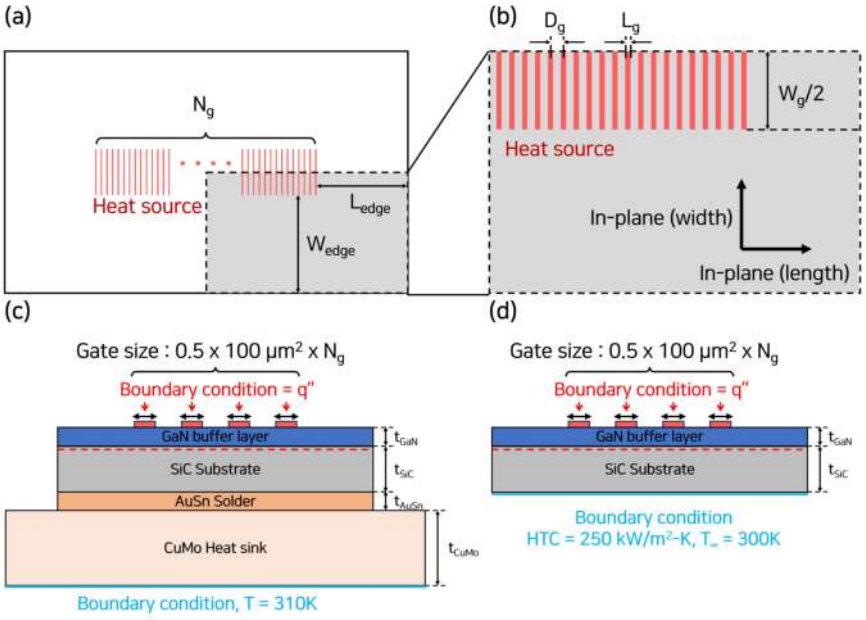

Figure 1. (a) Schematic of GaN-on-SiC HEMT device. (b) Images of heat source geometry. (c) Full package model and boundary conditions for simulation. (d) Simplified model and boundary conditions.

The gate-to-gate pitch (D_g) was set to 30 μm, and the heat source, representing the heat generation region between the gate and drain within the 2-dimensional electron gas layer of the actual device, was modeled as a rectangular shape [9–12]. The width (W_g) and length (L_g) of the heat source, indicating the hotspot for each gate finger, were set to 0.5 and 100.0 μm, respectively.

To account for heat flow from the edge gate to the device boundary, devices with different gates were modeled with varying overall device sizes. The width of the device boundary from the gate peripheral edge (W_{edge}) was set to 200 μm in all cases, while the length from the device boundary to the gate peripheral edge (L_{edge}) was fixed at 612.5 μm. The dimensions of the simulated device geometries are summarized in Table I. The overall device geometries and the dimensions of the heat sources are depicted schematically in Figs. 1(a) and 1(b) and the three-dimensional (3D) domain used for the simulation is illustrated in Fig. 1(c).

We first constructed a full-package 3D domain consisted of a 2 μm-thick GaN buffer layer, a 100 μm-thick SiC substrate, a 25 μm-thick AuSn solder, and a 14 × 4 mm^2 CuMo heat sink, arranged in descending order. An interfacial layer of a few nanometers, formed during the epitaxial growth of the GaN epi-layer on the SiC substrate, was replaced by a thermal boundary resistance (TBR) between the GaN layer and the SiC substrate. The TBR value used in this study was 30 m^2·K/GW, a commonly reported value for GaN-on-SiC devices [13]. To reduce computational cost, only a quarter-symmetric domain was simulated.

Heat sources were subjected to a power density P = 8 W/mm using a heat flux condition, and an isothermal boundary condition of 310 K was applied to the bottom surface of the CuMo heat sink. All other surfaces, except the heat sources and the bottom surface of the CuMo heat sink, were assigned adiabatic boundary conditions. The material properties used in the simulation were referenced from Sarua *et al.* [13] and are summarized in Table II.

Table I. Geometric parameters of the multi-finger GaN HEMT device.

Parameter	Definition	Value
W_{edge}	Width of heat source edge to chip edge	200 μm
L_{edge}	length of heat source edge to chip edge	612.5 μm
L_g	Length of heat source	100 μm
W_g	Width of heat source	0.5 μm
D_g	Gate to gate pitch	30 μm
N_g	Number of gates	2, 4, 12, 24
t_{GaN}	GaN buffer layer	2 μm
R_{TBR}	TBR	30 m^2-K/GW
t_{SiC}	SiC substrate layer	100 μm
t_{AuSn}	AuSn soldering	25 μm
t_{CuMo}	CuMo heat sink	1,000 μm

3. Results and discussion

To simplify the geometry, we replaced the AuSn soldering, and CuMo heatsink with a convective heat transfer boundary condition applied to the bottom of the SiC substrate instead of an isothermal boudary condition, as shown Fig. 1(d). Before conducting the simulations, a mesh independence test was performed, as shown in Fig. 2(a), to ensure convergence of the results. When a power density of P = 5 W/mm was applied to the heat source, the simulation was performed within a range of approximately 39 million hexahedral elements. Convergence was confirmed at around 30 million mesh elements, where the maximum temperature difference in the device was less than 0.2 °C. Fine mesh with a size of 125 nm was applied near the heat sources, where heat generation occurs, to accurately capture the temperature gradient.

Subsequently, the temperature results from the isothermal boundary condition at the bottom of the CuMo heat sink in the full-package model were used to determine the appropriate heat transfer coefficient, h for the simplified model applied to the bottom of the SiC substrate.

Table II. Material properties in the simulation [13].

Material	Thermal conductivity, k (W/m·K)	Heat capacitance, C_p (J/kg·K)	Mass density, ρ (kg/m^3)
GaN	$150\cdot(300/T)^{1.42}$	490	6,070
SiC	$420\cdot(300/T)^{1.3}$	1,200	3,200
AuSn	57	128	14,700
CuMo	167	134	9,900

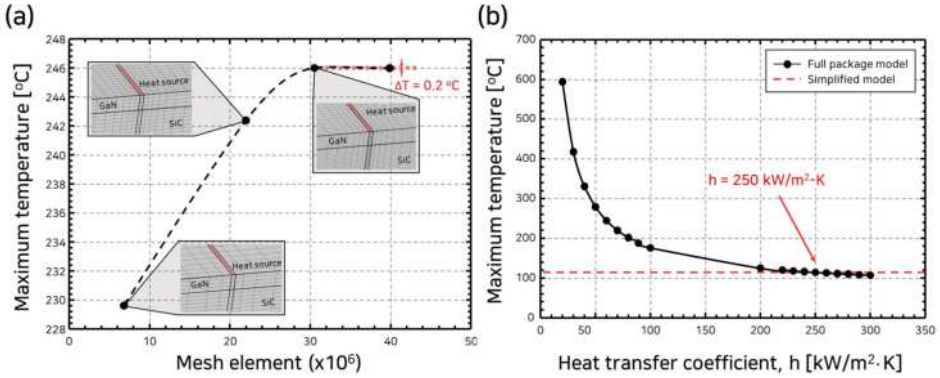

Figure 2. (a) Mesh independent test for each element size. (b) Maximum Temperature versus heat transfer coefficient *h* for simplified model.

The detailed process is illustrated in Fig. 2(b). As *h* increased from 5,000 to 300,000 W/m^2·K, the maximum temperature of the device decreased. Beyond 200 kW/m^2·K, the device temperature saturated, consistent with trends observed in previous studies on near-junction thermal transport for GaN-on-diamond substrates [9]. For the simplified model, a heat transfer coefficient of h = 250,000 W/m^2·K was applied, which resulted in a maximum device temperature of 114.05 °C, matching the full-package model.

Figures 3(a) and 3(b) illustrate the lateral and vertical temperature distributions, respectively, at P = 8 W/mm for devices with varying numbers of gate fingers. The device with 24 fingers exhibited the highest maximum temperature of 179.6 °C, while the 2-finger device had a significantly lower maximum temperature of 91.2 °C, representing a difference of 88.4 °C. Notably, the temperature difference between the maximum and minimum temperatures at the edges of the device was largest for the 24-finger device at 80.9 °C, which was 18.1 °C higher than the corresponding difference for the 12-finger device. These results indicate that as the number of fingers increases, thermal cross-talk intensifies near the device center, resulting in a larger temperature gradient between the center and the edges, thereby increasing temperature non-uniformity.

The vertical temperature distribution from the device surface to the SiC substrate, shown in Fig. 3(b), highlights the significant influence of TBR. Heat generated at the device surface is conducted through the SiC substrate and dissipated via convective cooling at the bottom of the substrate. However, the TBR, which naturally forms during the epitaxial growth of the GaN epi-layer on the SiC substrate, poses a major thermal bottleneck for heat conduction from the device surface to the SiC substrate. Depending on the number of fingers, the temperature difference across the TBR ranged from 13.5 to 18.4 °C. These emphasize the need to reduce the thermal resistance of the TBR to achieve efficient cooling.

As the current density increases, the heat generated in the device also increases, leading to a rise in the operating temperature. Figure 4 illustrates the temperature distributions of the device as a function of current density ranging 2 – 10 W/mm. For devices with a smaller number of fingers, such as the 2- and 4-finger device, the maximum temperature increases linearly with increasing current density. However, for devices with 12 and 24 fingers, the intensification of thermal cross-talk in the central region causes a nonlinear increase in the device temperature as the current density rises.

As both the current density and the number of fingers increase, the thermal cross-talk effect becomes more pronounced, causing a nonlinear rise in the device temperature, which ultimately makes stable operation impossible. Therefore, appropriate cooling technologies must be applied according to the device layout. Particularly, increasing the number of fingers is essential to enhance output power and transmission gain, necessitating advanced cooling techniques. According to Mudawar [14], h ranges for different cooling methods are as follows: natural convection (h = 5 – 1,200 W/m^2·K), single-phase cooling (h = 250 – 53,000 W/m^2·K), and two-phase cooling (h = 4,300 – 1,435,700 W/m^2·K).

By applying convective heat transfer boundary conditions with h ranging from 5,000 to 1,000,000 W/m^2·K to the bottom of the SiC substrate, the maximum device temperatures were analyzed and are shown in Fig. 5. For stable operation, the device temperature must remain below 200 °C. In regions with a red background, the device temperature becomes excessively high leading to device thermal-induced failure. Under air cooling methods, devices with 24 fingers exceed 200 °C and cannot operate stably. However, with direct convective cooling, increasing h shifts the 24-finger device into the blue region, indicating stable operation.

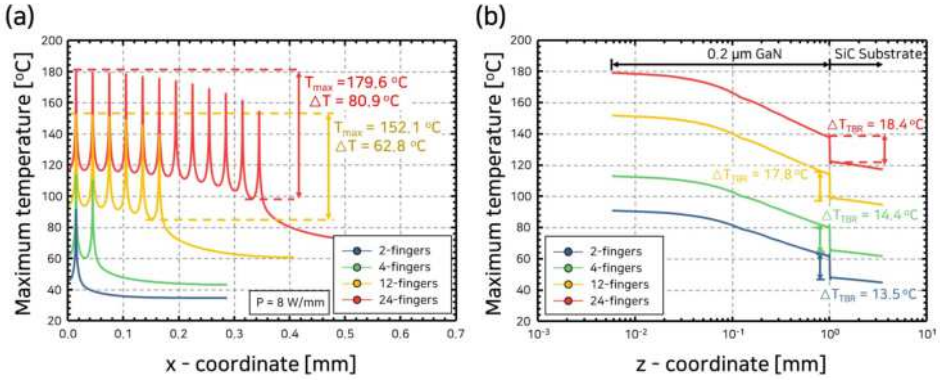

Figure 3. (a) Maximum temperature with different fingers at P = 8 W/mm along the horizontal x-coordinate. (b) Maximum temperature with different fingers at P = 8 W/mm along the vertical z-coordinate.

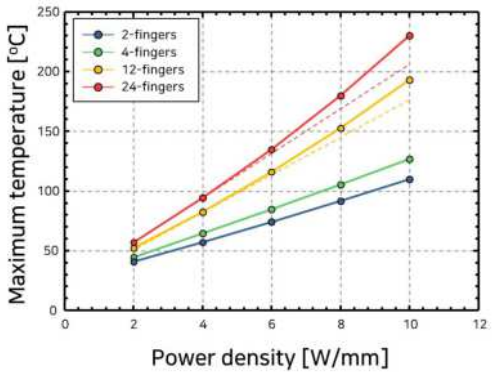

Figure 4. Maximum temperature versus power density *P* with different fingers.

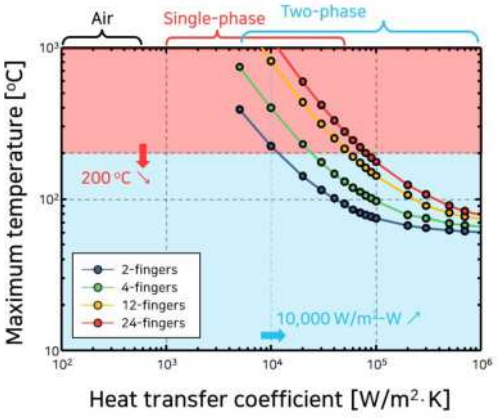

Figure 5. Maximum temperature versus heat transfer coefficient *h*. The range of typical heat transfer coefficients for air, single- and two-phase cooling is shown above.

To effectively lower the device temperature into the blue region, a heat transfer coefficient of at least 10,000 W/m^2·K is required. Implementing cooling techniques such as manifold microchannels on the backside of the SiC substrate can enable devices with significantly more fingers than 2-finger configurations to achieve high output power while maintaining stable operating temperatures.

4. Conclusions

In this study, the thermal cross-talk was investigated as a function of the number of gate fingers in GaN-on-SiC HEMT devices. Using the COMSOL Multiphysics v6.2 program, the maximum device temperatures were analyzed for simplified models with 2, 4, 12, and 24 fingers as the current density. At P = 8 W/mm, a comparison of the maximum device temperatures revealed that the 24-finger device reached 179.1 °C, whereas the 2-finger device reached 91.2 °C, indicating that the temperature rise due to thermal cross-talk in the central region became more pronounced as the number of fingers increased. Notably, the influence of TBR hindered efficient heat dissipation to the SiC substrate, especially in devices with a larger number of fingers.

For P = 2 – 10 W/mm, the device with 24 fingers exhibits a temperature range of 56.9 – 230.1 °C, while the device with 2 fingers shows a range of 40.7 – 109.9 °C. Therefore, it was determined that to operate a device with 24 fingers stably at temperatures below 200 °C, a high convective heat transfer coefficient of over 10,000 W/m^2·K is required.

Acknowledgments

This research was supported by Civil-Military Technology Cooperation Program (No. 19-CM-BD-05) and the National Research Foundation of Korea (NRF) grant funded by the Korea government (MSIT) (No. RS-2024-00353227).

Conflicts of Interest

The authors declare no conflicts of interest.

ORCID

Junrae Park https://orcid.org/0009-0001-4301-466x
Minsoo Kang https://orcid.org/0000-0003-4719-3076
Ilgyu Choi https://orcid.org/0000-0002-5566-3050
Hyun-Wook Jung https://orcid.org/0000-0001-5770-6387
Ho-Kyun Ahn https://orcid.org/0000-0003-3937-8257
Hyoungsoon Lee https://orcid.org/0000-0001-5961-6393

References

[1] Y. Dora, A. Chakraborty, L. Mccarthy, S. Keller, S. P. Denbaars, and U. K. Mishra, IEEE Electron Dev. Lett. 27, 713 (2006).
[2] T. Kabemura, S. Ueda, Y. Kawada, and K. Horio, IEEE Trans. Electron Dev. 65, 3848 (2018).
[3] B. Ridley, Brian Foutz, and L. Eastman, Phys. Rev. B 61, 16862 (2000).
[4] M. Haziq, S. Falina, A. A. Manaf, H. Kawarada, and M. Syamsul, Micromachines 13, 2133 (2022).
[5] K. J. Chen, Proceedings of the 2009 IEEE International Conference of Electron Devices and Solid-State Circuits (Xi'an, China, December 25-27, 2009).
[6] C.-Y. Su, M.-C. Tsai, and T.-L. Wu, Proceedings of the 2023 International VLSI Symposium on Technology, Systems and Applications (HsinChu, Taiwan, April 17-20, 2023).
[7] S. Yue *et al.*, IEEE Electron Dev. Lett. 43, 1199 (2022).
[8] I. G. Choi, S. J. Chnag, D. H. Kim, J. W. Lim, D. M. Kang, H. W. Jung, and H. K. Ahn, Appl. Sci. Converg. Technol. 33, 144 (2024).
[9] T. Y. Kim, C. H. Song, S. I. Park, S. H. Lee, B. J. Lee, and J. W. Cho, Int. Commun. Heat Mass Trans. 143, 106682 (2023).
[10] X. Chen, N. Donmezer, S. Kumar, and S. Graham, IEEE Trans. Electron Dev. 61, 4056 (2014).
[11] Y. J. Won, J. W. Cho, D. Agonafer, M. Asheghi, and K. E. Goodson, IEEE Trans. Comp. Packag. Manuf. Technol. 5, 737 (2015).
[12] M. T. Alam and M. M. Hasan, Proceedings of the 2021 5th International Conference on Electrical Engineering and Information Communication Technology (Dhaka, Bangladesh, November 18-20, 2021).
[13] A. Sarua, H. Ji, K. P. Hilton, D. J. Wallis, M. J. Uren, T. Martin, and M. Kuball, IEEE Trans. Electron Dev. 54, 3152 (2007).
[14] I. Mudawar, IEEE Trans. Comp. Packag. Technol. 24, 122 (2001).